ELSEVIER

Computer Physics Communications 118 (1999) 119–138

Computer Physics Communications

Implementation of time-dependent density functional response equations

S.J.A. van Gisbergen [a], J.G. Snijders [b], E.J. Baerends [a]

[a] *Section Theoretical Chemistry, Vrije Universiteit, De Boelelaan 1083, 1081 HV Amsterdam, The Netherlands*

[b] *Department of Chemical Physics and Materials Science Centre, Rijksuniversiteit Groningen, Nijenborgh 4, 9747 AG Groningen, The Netherlands*

Received 16 September 1998

Abstract

Time-dependent density functional theory provides a first principles method for the calculation of frequency-dependent polarizabilities, hyperpolarizabilities, excitation energies and many related response properties. In recent years, the molecular results obtained by several groups have shown that this approach is in general more accurate than the time-dependent Hartree–Fock approach, and is often competitive in accuracy with computationally more demanding conventional ab initio approaches. In this paper, our implementation of the relevant equations in the Amsterdam Density Functional program is described. We will focus on certain aspects of the implementation which are necessary for an efficient evaluation of the desired properties, enabling the treatment of large molecules. Such an efficient implementation is obtained by: using the full symmetry of the molecule, using a set of auxiliary functions for fitting the (zeroth- and first-order) electron density, using a highly vectorized and parallelized code, using linear scaling techniques, and, most importantly, by solving the response equations iteratively. © 1999 Elsevier Science B.V.

PACS: 31.15.Ew; 31.25.Jf; 33.15.Kr

Keywords: Density Functional Theory; Optical response properties of molecules

1. General introduction

In Density Functional Theory (DFT), based on the seminal papers by Hohenberg and Kohn [1] and Kohn and Sham [2], the electron density is obtained exactly from a single-particle equation for an electron moving in an effective field of the other electrons. This effective field can be subdivided into the Coulomb field of the nuclei, the Coulomb or Hartree term which comes from the Coulomb interaction of the electron with the electron density and finally, the unknown exchange-correlation (xc) potential. This xc potential contains all the many-body effects, and has to be approximated for practical applications. An important approximation is the Local Density Approximation (LDA), in which it is assumed that, locally, the quantum system under study can be approximated by a homogeneous electron gas. Although this might not seem appropriate for atoms and molecules, the LDA has been remarkably successful. More recently, the generalized gradient approximations (GGAs) have been developed. Instead of taking only the electron density into account, as in the LDA, the gradient of the density is also considered. This has led to important improvements in accuracy with respect to the LDA. With these functionals, accurate results for such properties as binding energies,

PII S0010-4655(99)00187-3

molecular geometries, and vibrational frequencies can be obtained.

However, ordinary DFT is restricted to ground-state problems. Excitation energy calculations within ground-state DFT are possible, through so-called ΔSCF techniques [3–6], but the theoretical basis is less solid than for ordinary ground-state properties, and several nontrivial theoretical complications make this approach less appealing than the time-dependent DFT approach to excitation energies described here. Important properties such as frequency-dependent polarizabilities and hyperpolarizabilities, their derivatives with respect to vibrational modes of the molecule, as well as Van der Waals dispersion coefficients, are either not at all accessible or not easily accessible through ground-state DFT. For this reason, the development of time-dependent DFT in the beginning of the previous decade [7–23] represented an important extension of DFT, for which the rigorous theoretical basis was given by Runge and Gross [24]. Until recently, however, calculations on frequency-dependent optical response were performed for atomic and solid state systems only.

This situation has changed by now, partly because of the growing interest of quantum chemists in DFT, partly because of the increasing know-how on molecular response calculations. At the moment, both by ourselves [25–33] and in other groups [34–45] implementations of the linear (and nonlinear) DFT response equations for molecules have been accomplished. In this work, our own implementation will be described. Because the applied techniques are not restricted to our own implementation, which we have named ADF-RESPONSE [46], but have also been used or can also be used in other codes, this work may also prove useful for improved understanding of other implementations.

The calculations can be split into two types in a natural way. The calculation of excitation energies and oscillator strengths is equivalent to the solution of an eigenvalue problem. The calculation of a frequency-dependent polarizability α or first hyperpolarizability β is equivalent to the solution of one or several sets of linear equations. Furthermore, the geometrical derivatives of these properties can be determined, by evaluating the derivatives through finite difference techniques, in which the response calculations are performed in a loop over different molecular geometries. The derivatives give access to such properties as Raman scattering [27,41], resonance Raman scattering, and hyper-Raman scattering. However, because the outer loop over molecular geometries poses no separate problems, our description will be limited to the two basic types of calculation mentioned above. For each of these, one has the choice between an iterative and a direct solution. As the iterative solution is less demanding both in memory and in CPU requirements, we will focus on the iterative approach. The direct solution of the eigenvalue or linear equations is feasible for small systems only.

In the quantum chemical programs in which the molecular time-dependent DFT calculations have been performed, one uses either Gaussian or Slater-type orbitals (GTOs or STOs), centered on the atoms. The GTOs have useful properties, which allow for an efficient, analytical evaluation of Coulomb type integrals. The STOs resemble the atomic orbitals more closely, because of their cusp at the nucleus and their slower decay in the outer region of the atom. For this reason, the number of STOs required for a calculation of a certain accuracy is usually considerably smaller than the number of GTOs. The Amsterdam Density Functional program (ADF) [47–49], in which our implementation of the response equations has been performed, uses STOs, in contrast to most other molecular DFT codes.

The one-particle eigenfunctions which appear in ground-state DFT are called the Kohn–Sham (KS) orbitals, being solutions to the KS equations. One can choose to evaluate the matrix elements which appear in the response equations between these KS orbitals (eigenfunctions) or between the primitive, atom-centered, GTO or STO basis orbitals, the Atomic Orbitals (AOs) which form the basis into which the KS orbitals are expanded. The first option has the advantage that the molecular symmetry can be fully exploited, with dramatic savings in memory and in CPU time for highly symmetric systems. The AO approach, on the other hand, provides the opportunity to make use of distance effects. This is due to the fact that integrals which depend on the overlap of two AOs centered on nuclei which are far apart are negligible and need not be calculated. This approach is therefore better suited for large systems of low symmetry. The advantages and disadvantages of both approaches will be discussed below, together with additional efficiency aspects of the implementation that have not yet been

mentioned.

The outline of the rest of this paper is as follows. First, the properties under consideration are briefly introduced, after which the theoretical basis of our approach, formed by the time-dependent Kohn–Sham (TDKS) equations in the density functional framework, is presented. We continue by introducing the linear response equations which can be obtained from a perturbative expansion of the TDKS equations, and which give access to the frequency-dependent polarizabilities and excitation energies. Finally we turn to a discussion of how these response equations can be solved efficiently, focusing on the matrix–vector multiplication which is the most time consuming part of both the excitation energy and polarizability calculations.

2. Description of desired properties

In this section, the properties we are trying to calculate are introduced. The molecular dipole moment μ_i in Cartesian direction i can be expanded in different orders of applied static external electric fields E_0^j, E_0^k, E_0^l, in directions j, k, l,

$$\mu_i = \mu_i^{(0)} + \alpha_{ij}E_0^j + \frac{1}{2!}\beta_{ijk}E_0^jE_0^k + \frac{1}{3!}\gamma_{ijkl}E_0^jE_0^kE_0^l + \dots , \quad (1)$$

where here, and in the following, summation over repeated indices is implied. The static linear polarizability tensor α, and the nonlinear polarizability tensors (hyperpolarizability tensors) β and γ have been introduced here, while $\mu_i^{(0)}$ is the ith component of the permanent dipole moment.

In the present paper we will be dealing mainly with the simplest and most important case, in which only the change in the *dipole* moment is considered due to perturbations of electric *dipole* fields. In a more complete formulation, one considers the effect of general multipolar electric fields, which act not only on the dipole moment, but also on the quadrupole, octupole, and higher multipole moments of the molecule. This leads to the definition of general multipole–multipole polarizabilities and hyperpolarizabilities. We have discussed the case of multipole–multipole polarizabilities in more detail in a previous paper [29], in which calculations of the more general multipole–multipole polarizabilities and the Van der Waals dispersion coefficients which are related to them have been presented. Here, we will restrict ourselves to the dipole case for the sake of readability.

If the applied electric fields are small, the magnitude of the change in the dipole moment depends linearly on the electric field strength, and the behavior of the system is consequently determined by the linear polarizability tensor α. For larger fields (for example strong laser fields), the first hyperpolarizability tensor β, the second hyperpolarizability tensor γ, and even higher-order tensors may become important. If the applied field becomes much larger still, the Taylor expansion does not converge anymore, and a nonperturbative approach is called for. A similar expansion as for the dipole moment could be given for the total energy, which is an equivalent formulation in case the so-called Hellmann–Feynman theorem [50,51] holds, which is the case in DFT.

The equation above is valid for static electric fields. In order to describe the usual experimental situation in which the external electric fields are frequency-dependent, the equation has to be extended. Expanding the dipole moment, which becomes time-dependent now, in orders of electric fields with a static and a frequency-dependent component $E = E_0 + E_\omega \cos(\omega t)$ in directions $i, j, k, \dots$, we get a more general form of the static equation above [52],

$$\begin{aligned}\mu_i(t) = {} & \mu_i^{(0)} \\ & + \alpha_{ij}(0;0)E_0^j + \alpha_{ij}(-\omega;\omega)E_\omega^j\cos(\omega t) \\ & + \tfrac{1}{2}\beta_{ijk}(0;0,0)E_0^jE_0^k + \tfrac{1}{4}\beta_{ijk}(0;\omega,-\omega)E_\omega^jE_\omega^k \\ & + \beta_{ijk}(-\omega;0,\omega)E_0^jE_\omega^k\cos(\omega t) \\ & + \tfrac{1}{4}\beta_{ijk}(-2\omega;\omega,\omega)E_\omega^jE_\omega^k\cos(2\omega t) + \cdots , \end{aligned} \quad (2)$$

where a widely used notation has been used for α and β. The frequencies after the semi-colon refer to the frequencies of the applied electric fields, while the sum of these frequencies is placed in front of the semi-colon, with a minus sign. The sum frequencies determine the time dependence of the dipole moment.

We note in passing that this expression is valid for molecular systems at small ω values, where no absorption occurs. In case absorption needs to be included in the treatment, for example in periodic systems, a generalization is needed in which also terms behaving

as $\sin(\omega t)$ occur, describing a time dependence of the dipole moment which is out of phase with the time dependence of the perturbation.

In first order, the dipole moment acquires a time dependence of the same frequency as the applied field. In higher order, more interesting effects become visible, such as Second Harmonic Generation (SHG), which is governed by the tensor $\beta(-2\omega;\omega,\omega)$, the final term in Eq. (2). In that case, the dipole moment oscillates with a frequency twice as high as the frequency of the external electric field.

The frequency-dependent polarizability is directly related to (vertical) excitation energies ω_i, oscillator strengths f_i, and transition dipole moments μ_i [53],

$$\alpha_{\mathrm{av}}(-\omega;\omega) = \sum_i \frac{f_i}{\omega_i^2-\omega^2} = \tfrac{2}{3}\sum_i \frac{\omega_i\mu_i^2}{\omega_i^2-\omega^2}\,, \quad (3)$$

where α_{av} is the average polarizability, equal to the average of the α_{xx}, α_{yy}, and α_{zz} components. From this equation it is clear that the poles of the polarizability tensor are directly related to the exact excitation energies. Although only the dipole-allowed and spin-allowed transitions have a nonzero contribution in this summation, the TDDFT approach allows the determination of triplet excitation energies, as well as excitation energies with zero oscillator strength. In the next section, the theoretical basis, upon which our determination of these properties rests, will be described.

3. The time-dependent Kohn–Sham equations

Ground-state DFT is based on the papers by Hohenberg and Kohn [1] and by Kohn and Sham [2]. The main result is that the density of a system is identical to the density of an associated noninteracting particle system moving in a *local* potential $v_s(\boldsymbol{r})$, defined by the Kohn–Sham equations (atomic units are used throughout)

$$\left[-\frac{\nabla^2}{2} + v_s[\rho](\boldsymbol{r})\right]\phi_i(\boldsymbol{r}) = \varepsilon_i\phi_i(\boldsymbol{r})\,. \quad (4)$$

Here the local potential $v_s[\rho](\boldsymbol{r})$ is the so-called Kohn–Sham potential, consisting of the external potential v_{ext} (the Coulomb field of the nuclei and external fields if present), the Hartree potential v_H, which is trivially calculated from the density, and the xc potential v_{xc}, which is the only unknown part,

$$v_s(\boldsymbol{r}) = v_{\mathrm{ext}}(\boldsymbol{r}) + v_H(\boldsymbol{r}) + v_{\mathrm{xc}}(\boldsymbol{r})\,. \quad (5)$$

The Kohn–Sham orbitals ϕ_i move in the effective field v_s, which depends upon the electron density $\rho(\boldsymbol{r})$. This density is exactly obtained by summing the squares of the Kohn–Sham orbitals and multiplying by their occupation numbers n_i,

$$\rho(\boldsymbol{r}) = \sum_i^{\mathrm{occ}} n_i|\phi_i(\boldsymbol{r})|^2\,. \quad (6)$$

As the KS potential $v_s(\boldsymbol{r})$ and the density $\rho(\boldsymbol{r})$ are interdependent, the equations have to be solved in a Self-Consistent Field (SCF) scheme, which means that one iteratively adapts the effective potential v_s and the density ρ until the difference in, for example, the energy between two subsequent cycles is sufficiently small. In the most straightforward fashion, this can be performed by mixing the density of the previous cycle with a (small) part of the density in the present cycle. This "simple damping" approach usually converges very slowly, and in practice the Direct Inversion in the Iterative Subspace (DIIS) procedure by Pulay and coworkers [54,55] is much to be preferred. In the DIIS approach, not only the result of the previous cycle, but the results of all, or many, previous cycles are taken into account, in order to obtain the optimal guess for the next cycle. If one is close to self-consistency, this procedure converges quadratically. Using DIIS, it typically takes about five to fifteen cycles to converge the SCF equations above.

In order to solve the KS equations, an approximation for the xc potential $v_{\mathrm{xc}}(\boldsymbol{r})$ is required, the simplest one being the LDA, based upon the local density of the system. The GGAs go beyond this and take the local gradient of the density into account as well, allowing for a much improved accuracy in the results for energies and geometries. Many other approximations, for example those based directly on the KS orbitals, are available.

The usual ground-state DFT scheme enables one to determine the density, and consequently the dipole moment, of a molecule with or without external electric fields. This affords the determination of the *static* polarizability and hyperpolarizability tensors α, β, and γ, by performing calculations in small electric fields of varying magnitudes and directions. In this so-called finite-field (FF) approach, the tensors are then determined from finite difference techniques. The main ad-

vantage of this approach is that no programming work is needed. Any standard DFT code will allow the determination of static properties in this manner. However, for the determination of higher-order tensors, such as γ, one needs very well-converged solutions to the KS equations in order to make reliable predictions, which may be technically hard to achieve and which will certainly lead to considerable increases in CPU time. A further disadvantage of this approach is the fact that results for many different electric fields have to be combined in case all components of a certain tensor are required, which, if not automated, costs additional human time.

The most fundamental disadvantage of the FF approach, however, is that one has access to static properties only. The *frequency-dependent* polarizability and hyperpolarizability tensors are not accessible. Excitation energies and oscillator strengths can also not be obtained from FF calculations. This is an important drawback of the FF approach, as it makes a direct comparison with experimental results impossible. Especially for hyperpolarizabilities it is known that there are substantial differences between the frequency-dependent and zero frequency results.

If one is interested in the time-dependent properties mentioned above, a time-dependent theory is required. In the DFT framework, this means that one has to start from the time-dependent KS (TDKS) equations as derived by Runge and Gross [24],

$$i\frac{\partial}{\partial t}\phi_i(\boldsymbol{r},t) = \left[-\frac{\nabla^2}{2} + v_s(\boldsymbol{r},t)\right]\phi_i(\boldsymbol{r},t) \equiv F_s\phi_i(\boldsymbol{r},t)\,. \tag{7}$$

The time-dependent KS potential $v_s(\boldsymbol{r},t)$ is subdivided in the same manner as its static counterpart,

$$v_s(\boldsymbol{r},t) = v_{\mathrm{ext}}(\boldsymbol{r},t) + v_H(\boldsymbol{r},t) + v_{\mathrm{xc}}(\boldsymbol{r},t)\,, \tag{8}$$

the Hartree potential being explicitly given by

$$v_H(\boldsymbol{r},t) = \int d\mathbf{r}'\,\frac{\rho(\boldsymbol{r}',t)}{|\boldsymbol{r}-\boldsymbol{r}'|}\,, \tag{9}$$

and the time-dependent xc potential $v_{\mathrm{xc}}[\rho](\boldsymbol{r},t)$ being an unknown functional of the time-dependent density $\rho(\boldsymbol{r},t)$, now given by

$$\rho(\boldsymbol{r},t) = \sum_i^{\mathrm{occ}} n_i \mid \phi_i(\boldsymbol{r},t) \mid^2\,. \tag{10}$$

If a certain approximation for the time-dependent xc potential $v_{\mathrm{xc}}(\boldsymbol{r},t)$ has been chosen, the TDKS equations can be solved iteratively, to yield the time-dependent density of a system, which may be exposed to an external time-dependent electric field. If one is interested in effects due to extremely large laser fields, the perturbative expansion of the dipole moment becomes meaningless, and the TDKS equations have to be solved nonperturbatively. This has until now been performed for atoms, by Ullrich and Gross [56–58], and more recently also by others [59], and gives access to such effects as higher harmonic generation (HHG), which are not accessible in a perturbative approach. The drawback of this is that the calculations are very time consuming, forbidding the treatment of medium-sized molecules. If one restricts oneself to properties which are accessible through perturbative methods, as we will do here, a much more efficient approach is possible, allowing the treatment of large molecules ($>$ 100 atoms). This approach will be the subject of the next section. For more information on time-dependent DFT in general, the reader is referred to the excellent reviews by Gross and coworkers [60,61,58]. A review paper which is more focussed on quantum chemistry is given by Casida [34].

4. Perturbative solution to time-dependent Kohn–Sham equations

The linear response equations which have to be solved can be presented in several equivalent ways [60,25,34,31]. Here, we adopt a notation close to that of our original paper [25] on the calculation of frequency-dependent polarizabilities and to that of Casida [34]. As we will focus mainly on efficiency matters in this work, only the first-order perturbed equations will be discussed. In another paper [31], we have indicated in detail how the first hyperpolarizability tensors $\beta_{ijk}(-\omega_\sigma;\omega_j,\omega_k)$ can immediately be obtained from the solutions to these first-order equations. The techniques which are needed for the determination of the hyperpolarizabilities are the same as those for the polarizabilities discussed here.

As our working equations have been derived from first principles several times [60,61,58,25,34], these equations will be presented without derivation, after

which the most time consuming parts of the calculations will be discussed in detail. In the following, real orbitals will be used and the complex conjugate signs will be discarded. Although the spin index σ will be kept at the start, the discussion will later be narrowed down to the spin-restricted case where $\phi_{i\uparrow}(\boldsymbol{r}) = \phi_{i\downarrow}(\boldsymbol{r})$. In this manner, it will be easier to focus on those aspects of the theory which are relevant to the present discussion.

For a linear polarizability calculation, the first-order change in the time-dependent density ρ_σ, of the spin σ electrons, which will depend on the frequency ω of the external electric field, has to be determined. In terms of products of occupied KS orbitals $\phi_{i\sigma}(\boldsymbol{r})$ with virtual KS orbitals $\phi_{a\sigma}(\boldsymbol{r})$, the first-order density can be written as

$$\rho_\sigma^{(1)}(\boldsymbol{r},\omega) = \sum_{i,a} [\, P_{ia}^\sigma(\omega)\phi_{a\sigma}(\boldsymbol{r})\phi_{i\sigma}(\boldsymbol{r}) + P_{ai}^\sigma(\omega)\phi_{a\sigma}(\boldsymbol{r})\phi_{i\sigma}(\boldsymbol{r})\,] \,, \tag{11}$$

P being the first-order density matrix on eigenfunction basis. As the zeroth-order density of Eq. (6) (the converged SCF density which comes out of an ordinary ground-state DFT calculation) only contains products of occupied orbitals, the first-order density can be written exclusively in terms of products of occupied and virtual orbitals. For this reason, only components P_{ai} or P_{ia} are nonzero and have been included in the summation (where, at variance with our earlier work [25], we have adopted the usual convention that a denotes a virtual orbital, while i stands for an occupied orbital). Using the expansion of the KS orbitals in the AO basis [$\phi_{i\sigma}(\boldsymbol{r}) = \sum_\mu C_{\mu i}^\sigma \chi_\mu(\boldsymbol{r})$], the first-order density can also be transformed to AO basis,

$$\rho_\sigma^{(1)}(\boldsymbol{r},\omega) = \sum_{\mu\nu} P_{\mu\nu}^\sigma(\omega)\chi_\mu(\boldsymbol{r})\chi_\nu(\boldsymbol{r}) \,. \tag{12}$$

Later, we shall show that the scaling of the calculations can be improved from N^4 to N^3 by making use of an additional set of functions $\{f_i\}$, called the auxiliary basis set or fit set, in terms of which $\rho_\sigma^{(1)}$ can be expressed as

$$\rho_\sigma^{(1)}(\boldsymbol{r},\omega) \approx \sum_1 a_i^\sigma(\omega) f_i(\boldsymbol{r}) \,. \tag{13}$$

All three expressions for the first-order density will be used. It should be emphasized that Eqs. (11) and (12) are equivalent, while an additional approximation is introduced in Eq. (13). The severity of this approximation depends upon the quality of the fit set (which, like the AO basis, is an atom-centered set of STOs in our case).

By expanding the KS equations to first order in the applied field, it can be shown that the first-order density, as determined by the density matrix elements in KS orbital basis, can be obtained from the solution of the following set of linear equations for the density matrix elements P_{jb}^σ and P_{bj}^σ [34,43,62],

$$\begin{aligned} &\sum_{jb\tau} \left[\delta_{\sigma\tau}\delta_{ij}\delta_{ab}(\varepsilon_{a\sigma} - \varepsilon_{i\sigma} + \omega) + K_{ia\sigma,jb\tau}\right] P_{jb}^\tau \\ &\quad + \sum_{jb\tau} K_{ia\sigma,bj\tau} P_{bj}^\tau = -\,[\delta v_{\text{ext}}]_{ia\sigma} \,, \\ &\sum_{jb\tau} \left[\delta_{\sigma\tau}\delta_{ij}\delta_{ab}(\varepsilon_{a\sigma} - \varepsilon_{i\sigma} - \omega) + K_{ai\sigma,bj\tau}\right] P_{bj}^\tau \\ &\quad + \sum_{jb\tau} K_{ai\sigma,jb\tau} P_{jb}^\tau = -\,[\delta v_{\text{ext}}]_{ai\sigma} \,, \end{aligned} \tag{14}$$

where δ_{ij} is the Kronecker delta, ω is the frequency of the applied field, $\varepsilon_{a\sigma}$ and $\varepsilon_{i\sigma}$ are KS spin orbital energies, and where the matrix elements of the external electric fields are given by

$$\begin{aligned} [\delta v_{\text{ext}}]_{ia\sigma} &= [\delta v_{\text{ext}}]_{ai\sigma} \\ &= \int d\boldsymbol{r}\, \phi_{i\sigma}(\boldsymbol{r})\delta v_{\text{ext}}(\boldsymbol{r})\phi_{a\sigma}(\boldsymbol{r}) \,. \end{aligned} \tag{15}$$

The external potential can be of general multipole form, labeled with the quantum numbers l and m [29],

$$\delta v_{\text{ext}}^{lm}(\boldsymbol{r},\omega) = \sqrt{\frac{4\pi}{2l+1}}\, E r^l Z_{lm}(\hat{r}) \cos(\omega t) \,, \tag{16}$$

where the function Z_{lm} stands for a real combination of spherical harmonics Y_{lm}. In the present paper, we will restrict ourselves to the dipole case ($l = 1$), for which the functions Z_{lm} simply reduce to x, y, and z.

The four-index matrix K, the so-called coupling matrix, consists of a Coulomb (or Hartree) part and an xc part,

$$K_{ij\sigma,kl\tau} = K_{ij\sigma,kl\tau}^{\text{Coul}} + K_{ij\sigma,kl\tau}^{\text{xc}} \,, \tag{17}$$

given by

$$K^{\mathrm{Coul}}_{ij\sigma,kl\tau} = \int d\boldsymbol{r} \int d\boldsymbol{r}'\, \phi_{i\sigma}(\boldsymbol{r})\phi_{j\sigma}(\boldsymbol{r}) \times \frac{1}{|\,\boldsymbol{r}-\boldsymbol{r}'\,|}\phi_{k\tau}(\boldsymbol{r}')\phi_{l\tau}(\boldsymbol{r}')\,, \tag{18}$$

and

$$K^{\mathrm{xc}}_{ij\sigma,kl\tau}(\omega) = \int d\boldsymbol{r} \int d\boldsymbol{r}'\, \phi_{i\sigma}(\boldsymbol{r})\phi_{j\sigma}(\boldsymbol{r}) \times f^{\sigma\tau}_{\mathrm{xc}}(\boldsymbol{r},\boldsymbol{r}',\omega)\phi_{k\tau}(\boldsymbol{r}')\phi_{l\tau}(\boldsymbol{r}')\,. \tag{19}$$

Here, we have introduced the Fourier-transform of the so-called xc kernel f_{xc}, which is the functional derivative of the time-dependent xc potential for the spin-σ electrons $v^{\sigma}_{\mathrm{xc}}(\boldsymbol{r},t)$ with respect to the time-dependent density of the spin-τ electrons $\rho_{\tau}(\boldsymbol{r}',t')$,

$$f^{\sigma\tau}_{\mathrm{xc}}(\boldsymbol{r},\boldsymbol{r}',t-t') = \frac{\delta v^{\sigma}_{\mathrm{xc}}(\boldsymbol{r},t)}{\delta\rho_{\tau}(\boldsymbol{r}',t')}\,. \tag{20}$$

This kernel determines the first-order change in the time-dependent xc potential due to the applied electric perturbation. In this work, we will restrict ourselves to the so-called Adiabatic LDA (ALDA) to this kernel, in which this complicated functional is reduced to a spatially local, frequency-independent, real function, evaluated at the local SCF density $\rho_0(\boldsymbol{r})$,

$$f^{\mathrm{ALDA},\sigma\tau}_{\mathrm{xc}}(\boldsymbol{r},\boldsymbol{r}',\omega) = \delta(\boldsymbol{r}-\boldsymbol{r}')\ \left.\frac{dv^{\mathrm{LDA},\sigma}_{\mathrm{xc}}}{d\rho_{\tau}}\right|_{\rho_{\tau}=\rho_{0,\tau}(\boldsymbol{r})}\,. \tag{21}$$

In the adiabatic approximation it is assumed that the functional derivative in Eq. (20) is nonzero only for $t = t'$, which can only be expected to be true for slow time-dependent processes. Practice shows however [30] that the adiabatic approximation is probably much less severe than other approximations, such as the approximation for the ground-state xc potential, which determines the KS orbitals ϕ_i and one-electron energies ε_i, and the other approximation in Eq. (21), namely the approximation of spatial locality, which is not present in more elaborate approximations for the xc kernel [63].

We consider the response due to a real spin-independent external perturbation δv_{ext}. If we restrict ourselves to the real density response (which is sufficient for (hyper)polarizabilities, excitation energies, and oscillator strengths) it is possible to simplify Eqs. (14) considerably by making use of the symmetry properties of the coupling matrix K. In case the ALDA is used one has that, because of the choice for real KS orbitals, $K_{ia\sigma,jb\tau} = K_{ia\sigma,bj\tau}$. The set of equations (14) can be transformed in a set of equations for $P^{\tau}_{jb} + P^{\tau}_{bj}$ and $P^{\tau}_{jb} - P^{\tau}_{bj}$ by respectively adding and subtracting the two equations. By combining the new coupled equations, the equation for the real density response is obtained. All this proceeds in a manner quite similar to time-dependent Hartree–Fock theory [64,65] and can be written down in the familiar time-dependent Hartree–Fock language [34,43]. Using the equality $K_{ia\sigma,jb\tau} = K_{ia\sigma,bj\tau}$, one obtains (after some algebra) for the real parts $\mathrm{Re}\,\delta P^{\tau}_{jb} = 1/2(P^{\tau}_{jb} + P^{\tau}_{bj})$ of the density matrix elements,

$$\sum_{bj\tau}\left[\delta_{\sigma\tau}\delta_{ab}\delta_{ij}(\varepsilon_i-\varepsilon_a) - 2K_{ia\sigma,jb\tau} - \omega^2\frac{\delta_{\sigma\tau}\delta_{ab}\delta_{ij}}{(\varepsilon_i-\varepsilon_a)}\right](\mathrm{Re}\,\delta P^{\tau}_{jb})(\omega) = [\delta v_{\mathrm{ext}}(\omega)]_{ia\sigma}\,, \tag{22}$$

which can be written in vector notation as

$$[\Delta - 2K](\mathrm{Re}\,\delta P) = \delta v_{\mathrm{ext}}\,, \tag{23}$$

where the matrix Δ is a trivial diagonal matrix: $\Delta_{ia\sigma,jb\tau} = \delta_{\sigma\tau}\delta_{ij}\delta_{ab}\left[(\varepsilon_i-\varepsilon_a) - \omega^2/(\varepsilon_i-\varepsilon_a)\right]$. It is important to stress that this matrix equation is now half the size of the previous ones in Eq. (14), with vectors of length $N_{\mathrm{occ}} \times N_{\mathrm{virt}}$ instead of $2N_{\mathrm{occ}} \times N_{\mathrm{virt}}$ (N_{occ} and N_{virt} being equal to the number of occupied and virtual orbitals, respectively). This makes the TDDFT response equations simpler than the related TDHF equations for which the equality $K_{ia\sigma,jb\tau} = K_{ia\sigma,bj\tau}$ does not hold [34].

The real part of the first-order density matrix P, obtained from the solution of the linear equations (23), gives access to the frequency-dependent polarizability [60,25,66]. At an excitation energy, a finite external perturbation δv_{ext} leads to an infinite change in the density matrix P in Eq. (23). This implies that the matrix $\Delta - 2K$ will possess a zero eigenvalue at the excitation energy. This leads, after a unitary transformation, to the following eigenvalue equation from which the excitation energies and oscillator strengths can be obtained [34,37,62],

$$\Omega\mathbf{F}_i = \omega_i^2\mathbf{F}_i\,, \tag{24}$$

where the components of the four-index matrix Ω are given by

$$\Omega_{ia\sigma,jb\tau} = \delta_{\sigma\tau}\delta_{ij}\delta_{ab}(\varepsilon_a - \varepsilon_i)^2 + 2\sqrt{(\varepsilon_a - \varepsilon_i)}K_{ia\sigma,jb\tau}\sqrt{(\varepsilon_b - \varepsilon_j)}\,. \quad (25)$$

The desired excitation energies are equal to ω_i, and the oscillator strengths are obtained from the eigenvectors $\mathbf{F}_i$ [34]. For a spin-restricted calculation, the Ω-matrix can be split in two separate singlet and triplet parts Ω^{S} and Ω^{T}, by performing a unitary transformation on the density matrix elements P_{ia}^{σ} [43,67,62],

$$u_{ia} = \frac{1}{\sqrt{2}}\left(P_{ia}^{\uparrow} + P_{ia}^{\downarrow}\right),$$
$$v_{ia} = \frac{1}{\sqrt{2}}\left(P_{ia}^{\uparrow} - P_{ia}^{\downarrow}\right), \quad (26)$$

in which spin-flip processes (for the triplet excitation energies) are separated from the processes which keep the total spin unchanged (singlet excitation energies). This leads to the following forms for the singlet and triplet Ω-matrices [67,43,62],

$$\Omega^{\mathrm{S}}_{ia,jb} = \delta_{ij}\delta_{ab}(\varepsilon_a - \varepsilon_i)^2 + 2\sqrt{(\varepsilon_a - \varepsilon_i)} \times 2[K^{\mathrm{Coul}}_{ia,jb} + \tfrac{1}{4}(f_{\mathrm{xc}}^{\uparrow\uparrow} + f_{\mathrm{xc}}^{\downarrow\downarrow} + f_{\mathrm{xc}}^{\downarrow\uparrow} + f_{\mathrm{xc}}^{\uparrow\downarrow})] \times \sqrt{(\varepsilon_b - \varepsilon_j)}\,,$$
$$\Omega^{\mathrm{T}}_{ia,jb} = \delta_{ij}\delta_{ab}(\varepsilon_a - \varepsilon_i)^2 + 2\sqrt{(\varepsilon_a - \varepsilon_i)} \times 2[\tfrac{1}{4}(f_{\mathrm{xc}}^{\uparrow\uparrow} + f_{\mathrm{xc}}^{\downarrow\downarrow} - f_{\mathrm{xc}}^{\downarrow\uparrow} - f_{\mathrm{xc}}^{\uparrow\downarrow})]\sqrt{(\varepsilon_b - \varepsilon_j)}, \quad (27)$$

where $f_{\mathrm{xc}}^{\sigma\tau}$ stands for the functional derivative $\delta v_{\mathrm{xc}}^{\sigma}/\delta\rho_{\tau}$, and where $\frac{1}{4}(f_{\mathrm{xc}}^{\uparrow\uparrow} + f_{\mathrm{xc}}^{\downarrow\downarrow} + f_{\mathrm{xc}}^{\downarrow\uparrow} + f_{\mathrm{xc}}^{\uparrow\downarrow})$ is equal to the spin-restricted kernel $f_{\mathrm{xc}} = \delta v_{\mathrm{xc}}/\delta\rho$. The triplet equivalent $\frac{1}{4}(f_{\mathrm{xc}}^{\uparrow\uparrow} + f_{\mathrm{xc}}^{\downarrow\downarrow} - f_{\mathrm{xc}}^{\downarrow\uparrow} - f_{\mathrm{xc}}^{\uparrow\downarrow})$ is usually named G_{xc} [67] and can be obtained from the derivative of the xc energy density of the homogeneous electron gas with respect to the spin-polarization parameter ζ [67–69]. These singlet and triplet matrices can be diagonalized separately. For a spin-unrestricted calculation, a similar procedure would give rise to more general spin states, but that case is not considered here.

Let us consider the equations for the excitation energies and for the polarizability in more detail. In both cases, a direct solution is possible in principle. This requires calculating and storing all matrix elements of the coupling matrix K, however. For this four-index matrix, this implies storing $N_{\mathrm{occ}}^2 \times N_{\mathrm{virt}}^2$ matrix elements, which becomes unfeasible for a typical calculation with more than 1000 basis functions. Apart from the memory requirements, the CPU time also gets out of hand with this approach. Both the solution of the set of linear equations and the solution of the eigenvalue problem would require a number of floating point operations which would scale as $N_{\mathrm{occ}}^3 \times N_{\mathrm{virt}}^3$. Again, this is very forbidding for large molecules or basis sets.

An alternative and preferable approach is to solve the equations iteratively, as was already stressed by Olsen and coworkers [70] for the similar (multiconfiguration) Hartree–Fock case. For the solution of the linear equations, one typically uses conjugate gradient techniques. We have previously explained the details of our approach [25], which is based upon the DIIS procedure [54,55] mentioned above, also used in the iterative solution for the ground-state KS equations [49]. For the iterative solution of the eigenvalue equation, one has to make a restriction to a few selected eigenvalues, usually the lowest excitation energies. We employ the Davidson algorithm [71–73], which has been shown to be very efficient [70]. One particular implementation of this algorithm has earlier been described in this journal [74].

In the iterative solution for the polarizability, one tries to find accurate trial vectors for the density matrix P, which solve the set of linear equations (14) to within a certain threshold. For the eigenvalue equation in Eq. (24), the aim is to find accurate approximations to the eigenvectors $\mathbf{F}_i$. In both cases an initial guess for P or $\mathbf{F}_i$ is needed. One can use the approximation $K = 0$ as a reliable starting point. For the polarizability calculation this initial guess for the density matrix yields the so-called "uncoupled" polarizability, which is usually a fair estimate of the converged result, the "coupled" polarizability. In the excitation energy calculation, the excitation energies in the first cycle are equal to the differences between eigenvalues of occupied and unoccupied KS orbitals. This is known [75] to be a good approximation in many cases, and is explicitly used as a "zeroth-order" approximation for the excitation energy in the approach by Petersilka and Gross [63,67].

Both iterative procedures require the results of repeated matrix–vector multiplications (in our case the matrix is K, the diagonal Δ-matrix being trivial), without the need for storing or even knowing the individual matrix elements. The key problem has thus been reduced to the construction of an efficient routine for

performing the matrix–vector multiplication $K \cdot p$. The efficient implementation of such a matrix–vector multiplier is the subject of the following section.

5. Efficient implementation of matrix–vector multiplication

As mentioned, almost all of the CPU time in the response calculations resides in the matrix–vector multiplication $K \cdot p$, where K is the square coupling matrix, with Coulomb and xc parts, and p is a vector of length $N_{\mathrm{occ}} \times N_{\mathrm{virt}}$. This matrix–vector product occurs both in the equations for the excitation energies and oscillator strengths and in the equations for the polarizability. The efficient evaluation of this product is discussed in the following subsections, each dealing with a separate aspect of improving the efficiency. The use of auxiliary basis functions, the use of molecular symmetry, use of parallelization techniques, as well as prescreening, cutoff, and linear scaling techniques, are discussed in this order.

5.1. Use of auxiliary basis functions

The matrix–vector product $\boldsymbol{p}_{\mathrm{out}} = K \cdot \boldsymbol{p}_{\mathrm{in}}$ under consideration, has the following form:

$$\begin{aligned}[p_{\mathrm{out}}]_{ia} &= \sum_{jb} K_{ia,jb}[p_{\mathrm{in}}]_{jb} \\ &= \sum_{jb} \int d\boldsymbol{r} \int d\boldsymbol{r}' \phi_i(\boldsymbol{r})\phi_a(\boldsymbol{r}) \\ &\quad \times \left[\frac{1}{|\,\boldsymbol{r}-\boldsymbol{r}'\,|} + f_{\mathrm{xc}}^{\mathrm{ALDA}}(\boldsymbol{r})\delta(\boldsymbol{r}-\boldsymbol{r}') \right] \\ &\quad \times \phi_j(\boldsymbol{r}')\phi_b(\boldsymbol{r}')[p_{\mathrm{in}}]_{jb} \,. \end{aligned} \tag{28}$$

The first step is to define the density $\rho_{\mathrm{in}}(\boldsymbol{r}) = \sum_{jb}[p_{\mathrm{in}}]_{jb}\phi_j(\boldsymbol{r})\phi_b(\boldsymbol{r})$ and transform it to the AO basis, by using the expansion of the KS orbitals ϕ_j and ϕ_b in this basis,

$$\phi_j(\boldsymbol{r}) = \sum_{\mu} C_{\mu j}\chi_{\mu}(\boldsymbol{r}) \,. \tag{29}$$

In this way, the density ρ_{in} can be written in terms of an AO density matrix P^{in},

$$\rho_{\mathrm{in}}(\boldsymbol{r}) = \sum_{\mu\nu} \left[P^{\mathrm{in}}\right]_{\mu\nu} \chi_{\mu}(\boldsymbol{r})\chi_{\nu}(\boldsymbol{r}) \,, \tag{30}$$

where the AO density matrix coefficients $[P^{\mathrm{in}}]_{\mu\nu}$ are known in terms of the AO coefficients $C_{\mu j}$. The transformation from the KS basis to the AO basis is not very time consuming, provided that it is performed in two separate steps, where the first step consists of a transformation to a mixed basis representation of AOs and occupied orbitals.

At this point, nothing has been gained, as one still needs to go through four loops: those over i, a, μ, and ν, resulting in an N^4 algorithm. However, by fitting the density, the loops over μ and ν can be replaced by a single loop over the fit functions f_i, improving the scaling to N^3,

$$\rho_{\mathrm{in}}(\boldsymbol{r}) \approx \tilde{\rho}_{\mathrm{in}}(\boldsymbol{r}) = \sum_i a_i f_i(\boldsymbol{r}) \,. \tag{31}$$

In the RESPONSE part of the ADF program, the density fit is performed in the same manner as for the zeroth-order density. First, the density is split in atom pair densities, for which the AO representation is needed. Then this atom pair density is fitted with fit functions which are centered on the two atoms in the pair. This fit per atom pair ensures that the fitting procedure scales as N^2 with increasing system size. The fit coefficients a_i are determined from the requirement that the integrated squared difference between the true atom pair densities $\rho_{\mathrm{at.p.}}$ and the fitted densities $\tilde{\rho}_{\mathrm{at.p.}}$,

$$\int d\boldsymbol{r} \left[\rho_{\mathrm{at.p.}}(\boldsymbol{r}) - \tilde{\rho}_{\mathrm{at.p.}}(\boldsymbol{r})\right]^2 \,, \tag{32}$$

should be minimal, under the constraint that the total atom pair charge remains unchanged. The quality of the fit can be controlled by adding suitable functions to the fit set, and checked by calculating the difference integral of Eq. (32). More details about the fitting procedure in ADF can be found in Refs. [47,76]. Using this fitted density, the expression for the matrix–vector product becomes

$$\begin{aligned}\sum_{jb} K_{ia,jb}[p_{\mathrm{in}}]_{jb} &= \int d\boldsymbol{r}\, \phi_i(\boldsymbol{r})\phi_a(\boldsymbol{r}) \\ &\quad \times \int d\boldsymbol{r}' \left[\frac{1}{|\,\boldsymbol{r}-\boldsymbol{r}'\,|} + f_{\mathrm{xc}}^{\mathrm{ALDA}}(\boldsymbol{r})\delta(\boldsymbol{r}-\boldsymbol{r}') \right] \\ &\quad \times \sum_i a_i f_i(\boldsymbol{r}') \,. \end{aligned} \tag{33}$$

This equation is of the form

$$[p_{\text{out}}]_{ia} = \int d\boldsymbol{r}\, \phi_i(\boldsymbol{r})[v_{\text{ind}}(\boldsymbol{r})]\phi_a(\boldsymbol{r}) , \tag{34}$$

where the induced potential $[v_{\text{ind}}]$ has been introduced. We use this description because the induced potential depends upon the density change ρ_{in} which is induced by the external perturbation. The induced potential is, in terms of the fitted density, given by

$$v_{\text{ind}}(\boldsymbol{r}) = \int d\boldsymbol{r}' \left[\frac{1}{|\boldsymbol{r}-\boldsymbol{r}'|} + f_{\text{xc}}^{\text{ALDA}}(\boldsymbol{r})\delta(\boldsymbol{r}-\boldsymbol{r}')\right] \times \sum_i a_i f_i(\boldsymbol{r}') . \tag{35}$$

The matrix elements of the induced potential v_{ind} in Eq. (34) are calculated by numerical integration. A separate section of the ADF program [48,77] determines the coordinates $\boldsymbol{r}_k$ and the weights w_k of the quadrature points, from the geometry of the molecule and the desired accuracy in the integrals, typically leading to a few thousand integration points per atom. The numerical integral evaluation for a general integrand $g(\boldsymbol{r})$ can be written as

$$\int g(\boldsymbol{r})\, d\boldsymbol{r} = \sum_k w_k g(\boldsymbol{r}_k) , \tag{36}$$

which, for the induced potential matrix elements, results in

$$\left[p_{\text{out}}\right]_{ia} = \sum_k w_k \phi_i(\boldsymbol{r}_k) v_{\text{ind}}(\boldsymbol{r}_k) \phi_a(\boldsymbol{r}_k) . \tag{37}$$

The two most expensive steps in the evaluation of the matrix–vector product are the evaluation of the potential v_{ind} in all the integration points $\boldsymbol{r}_k$ and the evaluation of the $N_{\text{occ}} \times N_{\text{virt}}$ numerical integrals occurring in Eq. (34). Each of these integrals requires an operation count which scales linearly with the total number of integration points for the molecule, N_{point}. The total CPU time involved in the evaluation of the integrals, once v_{ind} is known in the integration points, is proportional to $N_{\text{occ}} \times N_{\text{virt}} \times N_{\text{point}}$, where typically $N_{\text{point}} \gg N_{\text{virt}} > N_{\text{occ}}$.

For the integral calculation to be the time-determining step, one needs an efficient evaluation of the induced potential in the integration points. This proceeds as follows. As we use STOs for the fit functions, the Coulomb potential belonging to the fitted density can be obtained analytically [78],

$$v^{\text{Coul}}(\boldsymbol{r}) = \int d\boldsymbol{r}' \left[\frac{\sum_i a_i f_i(\boldsymbol{r}')}{|\boldsymbol{r}-\boldsymbol{r}'|}\right] = \sum_i a_i g_i(\boldsymbol{r}) , \tag{38}$$

where the functions g_i are known. The part of the induced potential involving the ALDA xc kernel is trivial, because of the delta function. In short, the induced potential is obtained as

$$\begin{aligned} v_{\text{ind}}(\boldsymbol{r}) &= \int d\boldsymbol{r}' \left[\frac{1}{|\boldsymbol{r}-\boldsymbol{r}'|} + f_{\text{xc}}^{\text{ALDA}}(\boldsymbol{r})\delta(\boldsymbol{r}-\boldsymbol{r}')\right] \times \sum_i a_i f_i(\boldsymbol{r}') \\ &= \sum_i a_i \left[g_i(\boldsymbol{r}) + f_{\text{xc}}^{\text{ALDA}}(\boldsymbol{r}) \times f_i(\boldsymbol{r})\right] , \end{aligned} \tag{39}$$

which leads to a favorable N^3 scaling.

5.2. Use of full molecular symmetry

Once the induced potential has been calculated in the integration points, one needs to calculate $N_{\text{occ}} \times N_{\text{virt}}$ integrals as in Eq. (34). As pointed out, the calculation time for this will be proportional to $N_{\text{occ}} \times N_{\text{virt}} \times N_{\text{point}}$. However, as one knows the transformation properties of all occupied and virtual orbitals (the irreducible representations (irreps) Γ to which they belong, as well as the columns α of these irreps are known), as well as the transformation properties of the external potential, and consequently the induced potential, group theory can be used to reduce the number of required operations considerably.

The savings are three-fold. In the first place, one does not need all the integration points of the molecule, but only those which belong to the symmetry-unique wedge, substantially reducing the cost *per integral*. This implies that N_{point} is reduced by a factor which is equal to the number of group operators (which, for example, is no less than 48 for the O_h symmetry). This is usually the most important gain in time, as the CPU time needed for the expensive calculation of the induced potential in the integration points is automatically reduced by the same factor.

In the second place, one can use the symmetry properties to minimize the *number* of integrals which need to be calculated. Already on the basis of the irreps to which the orbitals and the operator belong, one can predict many integrals to be zero. Entire blocks of in-

tegrals do not need to be calculated for this reason. The third saving is the most trivial one. Equivalent symmetry blocks (for the excitation energy calculations) or equivalent external fields (for the polarizability calculations) can (and should) be treated at the same time. This implies that, for example, the x and y directions of a molecule with cylinder symmetry around the z-axis can be treated simultaneously.

All this will be made more explicit below. In the following group theoretical approach, we follow Cornwell [79], although adopting a different notation. We consider the set of $N_{\mathrm{occ}} \times N_{\mathrm{virt}}$ integrals,

$$\int d\boldsymbol{r}\, \phi_i(\boldsymbol{r}) v(\boldsymbol{r}) \phi_a(\boldsymbol{r}) , \tag{40}$$

where ϕ_i and ϕ_a are KS orbitals, and the operator $v(\boldsymbol{r})$ is typically the induced potential. The KS orbitals occurring in this equation can be labeled by the irrep and column of the irrep to which they belong. In order to make full use of group theory, one has to ensure that the operators (or potentials) $v(\boldsymbol{r})$ can be labeled similarly. This can be done by choosing proper external perturbations δv_{ext} in Eq. (16), or proper symmetry-adapted trial vectors for $\mathbf{F}_i$ in an excitation energy calculation. For the external perturbations, this means that one treats linear combinations of the regular spherical harmonics (such as x, y, and z in the dipole polarizability case), instead of the spherical harmonics themselves, which does not affect the final results in any way. One furthermore has to make sure that the operators belonging to different columns of a multidimensional irrep q will transform as a set of *irreducible tensor operators* for that irrep, as defined in, for example, Ref. [79].

The matrix element for the specific KS orbitals i and a is nonzero only if it contains a part which transforms according to the A1 irrep, or, in other words, if it contains a part which is completely symmetrical. Furthermore, the value of the integral is identical to the contribution of its completely symmetrical part. One can easily establish whether or not an integral vanishes from the knowledge of the Clebsch–Gordan series, which specifies how the direct product of two irreps can be expressed in a direct sum of all irreps Γ^r of the symmetry group [79],

$$\Gamma^p \otimes \Gamma^q \approx \sum_r \oplus n^r_{pq} \Gamma^r . \tag{41}$$

In case the orbitals i and a transform according to the irreps Γ^p and Γ^q, respectively, the corresponding matrix element will vanish, unless the integer n^r_{pq} is nonzero, where Γ^r is the irrep the operator belongs to. Many point groups which describe the symmetry of molecules are *simply reducible*, meaning that n^r_{pq} is equal to 0 or 1 for all p, q, r. In such a case, the equations given below will simplify considerably.

If one considers products of basis functions $\{\phi^p_j\}$ belonging to irrep Γ^p (j denotes the column, in the range $l = 1 \ldots \dim(\Gamma^p)$) with basis functions $\{\psi^q_k\}$ of the irrep Γ^q, one obtains a set of $\dim(\Gamma^p) \times \dim(\Gamma^q)$ product functions, which, with the use of the Clebsch–Gordan coefficients $\langle \Gamma^p j, \Gamma^q k \mid \Gamma^r l\alpha \rangle$, can be symmetry-combined to $\alpha = 1 \ldots n^r_{pq}$ sets of functions $\theta^r_{l,\alpha}$ transforming according to column l of irrep Γ^r,

$$\theta^{r,\alpha}_l(\boldsymbol{r}) = \sum_{j=1}^{d_p} \sum_{k=1}^{d_q} \langle \Gamma^p j, \Gamma^q k \mid \Gamma^r l\alpha \rangle \, \phi^p_j(\boldsymbol{r}) \psi^q_k(\boldsymbol{r}) , \tag{42}$$

where d_p stands for the dimension of irrep Γ^p, and $\alpha = 1 \ldots n^r_{pq}$. For the most common case of simply reducible groups, this simplifies, as n^r_{pq} is always equal to zero or one. With the notation for the Clebsch–Gordan coefficients established, the Wigner–Eckart theorem can now be formulated. For a set of irreducible tensor operators Q^q_k, with irrep label q and column label k, the following relation holds for the matrix elements between orbitals ϕ^r_l and ψ^p_j [79]:

$$\left(\phi^r_l, Q^q_k \psi^p_j\right) = \sum_{\alpha=1}^{n^r_{pq}} \langle \Gamma^p j, \Gamma^q k \mid \Gamma^r l\alpha \rangle^* \times \left(r \,||\, Q^q \,||\, p\right)_\alpha . \tag{43}$$

In words, the theorem states that the values of the set of integrals $\left(\phi^r_l, Q^q_k \phi^p_j\right)$ can, in combination with the knowledge of the Clebsch–Gordan coefficients, be obtained for all values of j, k, and l from the possibly much smaller set of $\alpha = 1 \ldots n^r_{pq}$ "reduced matrix elements" $\left(r \,||\, Q^q \,||\, p\right)_\alpha$, which are independent of l, k, and j. The strategy is therefore to evaluate the reduced matrix elements in the cheapest possible manner and to obtain all desired nonzero matrix elements by multiplication with the appropriate Clebsch–Gordan coefficients, the determination of which is cheap. The

reduced matrix elements are obtained from the basic integrals,

$$\left(r \,||\, Q^q \,||\, p\right)_\alpha = \frac{1}{d_r} \sum_{j,k,l} \left(\phi_l^r, Q_k^q \phi_j^p\right) \times \left\langle \Gamma^q k, \Gamma^p j \mid \Gamma^r l \alpha \right\rangle . \tag{44}$$

It can be explicitly shown that the total integrand of the right-hand side of this equation is invariant under the $A1$-projector, which projects out the totally symmetric component. This implies that only the points in the irreducible wedge are needed for the evaluation of the reduced matrix elements. It is important to realize that this is not true for the individual basic integrals on the right-hand side, which are not necessarily totally symmetric. However, when multiplied by the Clebsch–Gordan coefficients and combined with the other contributions, the total (the reduced matrix element) will be totally symmetric. If one uses only points from the symmetry-unique wedge, the contribution of the individual basic integrals will consequently be calculated incorrectly, but the reduced matrix element will be correct. Afterwards, the basic integrals are obtained from the reduced matrix elements, as in Eq. (43). Needless to say, only the basic integrals will be calculated of which the associated Clebsch–Gordan coefficient is nonzero.

Summarizing this section, we can say that the use of symmetry permits a significant speed-up of the response calculations, mainly due to the fact that the number of integration points can be strongly reduced, but also due to the significantly smaller number of integrals which has to be evaluated. More details on the use of the full molecular symmetry in the ADF-RESPONSE code are available in the form of an internal report [80].

5.3. Parallelization

The major part of the CPU time depends linearly on the number of integration points N_{point}. Even if only the work which has to be performed in all integration points can be divided between different processors, a reasonably well parallelized code results already. In the ADF program, this is done as follows [49]. The total number of integration points is subdivided into N_{block} blocks, each with the same length L_{block}. This machine-dependent block length is chosen such that vectorization proceeds effectively.

The blocks are divided equally between the different processors (nodes). After this, each processor calculates the induced potential (the response operator) in its own blocks of integration points and determines the contribution from those blocks of integration points to the matrix elements. After all nodes are finished with their parts of the numerical integration, there will be communication between the nodes, in order to calculate the total value of the integrals. The transformations from AO to KS orbital basis and vice versa have also been parallelized in the ADF-RESPONSE code. This results in an overall parallelization of typically 99% of the ADF-RESPONSE code, which gives good speed-ups up to a considerable number of processors.

In ADF, a high-level portable parallelization library, the PP library, has been set up [49], which is based on the low-level routines of either the public-domain Parallel Virtual Machine (PVM) [81] or the Message Passing Interface (MPI) protocols. The high-level routines have been used for the parallelization of the ADF-RESPONSE code [46], implying that for the parallelization of this part of ADF, the same techniques have been used as for the rest of the ADF program. A detailed description of the parallelization of ADF, including timing results can be found in Ref. [49].

5.4. Distance effects and linear scaling techniques

Instead of calculating matrix elements between occupied and virtual KS orbitals, such as

$$\int d\boldsymbol{r}\, \phi_i(\boldsymbol{r}) [v_{\text{ind}}(\boldsymbol{r})] \phi_a(\boldsymbol{r}) , \tag{45}$$

it is also possible to calculate the AO matrix elements

$$\int d\boldsymbol{r}\, \chi_\mu(\boldsymbol{r}) [v_{\text{ind}}(\boldsymbol{r})] \chi_\nu(\boldsymbol{r}) , \tag{46}$$

and transform to eigenfunction basis afterwards. The disadvantage of this, so-called direct, approach is obvious. Even if no symmetry is present, the number of integrals which has to be evaluated is far bigger in the second case. If the number of primitive basis functions is N_{bas}, one needs to evaluate $N_{\text{bas}} \times (N_{\text{bas}} + 1)/2$ integrals, instead of $N_{\text{occ}} \times N_{\text{virt}}$, the latter number possibly being substantially smaller. If the symmetry is

high and the basis set is large, the difference in the number of integrals becomes huge.

For large molecules, which are usually nonsymmetric, the AO approach will become preferable however, because distance effects can be employed. Two AOs, centered on nuclei which are far apart, will have very small overlap, resulting in a negligible value for the integral of Eq. (46). In general, an AO will have nonvanishing overlaps with only a fixed number of AOs situated on close-lying atoms, inside a certain radius R. Because only integrals involving AOs on these neighbors need to be calculated, the number of integrals will, for large systems, scale linearly with the number of atoms. This is the desirable linear scaling which is aimed at in ground-state DFT calculations as well. Such linear scaling is not reached for the eigenfunction approach, as the KS orbitals are hardly ever localized on a few atoms, but are usually spread out over the entire molecule.

The use of distance effects can be applied at three levels [76]. In the outermost loop for the calculation of the KS matrix, which is the loop over atom pairs in ADF, those pairs of atoms can be skipped, for which all AOs centered on the two atoms of the pair have negligible overlap. The number of integrals which has to be evaluated scales linearly if this first step is implemented, but an efficient linear scaling of the entire calculation is only realized if two more steps are implemented.

For a certain atom pair, it is not necessary to evaluate matrix elements between all AOs on atom 1 and atom 2. Only those AO pairs for which the overlap matrix element $S_{\mu\nu} = \int d\boldsymbol{r}\, \chi_\mu(\boldsymbol{r})\chi_\nu(\boldsymbol{r})$ is larger than some threshold value need to be taken into account. This overlap matrix element is estimated from an approximation to the tails of the AOs. The third and final step is at the level of an individual integral. Each of the N_{block} blocks of integration points (each with L_{block}) points, has a contribution to the total integral, but for some blocks this contribution will be negligible. A simple criterion [44] for judging if a certain integration block needs to be taken into account, is to calculate the maximum value of the products of the AOs in the current block. This product can be used as a measure for the contribution of the current block of integration points and on the basis of its magnitude one can decide whether or not it is necessary to take that block into account. In ADF, a slightly different criterion is adopted, in which the weight of the tail of a function in a certain block determines whether or not the block should be taken into account [76].

In order for this final step to be useful, the spread in the values of the operator and the AOs in a certain block should not be too large. This requires blocks which are well localized in space and do not contain too many integration points. The latter demand implies using a relatively small value for L_{block}, conflicting with the demand for efficient vectorization, which requires a large L_{block} value.

Until now, we have discussed the evaluation of matrix elements only. However, one has to take care that the evaluation of the response operator is performed in a linear scaling fashion as well. If this is not done, this part of the calculation will dominate the total CPU time. To this purpose one can use several techniques, such as a multipole expansion for the Coulomb potential [76], but the discussion of these falls outside the scope of the present article.

Only a limited number of techniques which make use of distance effects have been implemented in the ADF-RESPONSE code [46] at present. The full implementation of linear scaling techniques and distance effects is left for future work, and will be performed along similar lines as the linear scaling implementation for the ground-state KS equations in ADF [76].

6. Selected molecular applications

In the following sections some of the results which have been obtained by ourselves and by others are discussed in order to highlight certain points which are important for practical applications, and to show what type of calculations are feasible with the present method and what accuracy can typically be reached.

6.1. *Influence of asymptotic behavior of* v_{xc}

The approximation which is made for the xc potential v_{xc} is very important for the accuracy of response calculations, as it determines the KS orbital energy differences and the KS orbitals, which provide the starting point for the response calculation. Apart from this approximation, the xc kernel f_{xc} has to be approximated, which can be chosen independently from the xc potential. In our applications described here, the

ALDA was used for the xc kernel and various xc potentials were used in the ground-state calculation.

It is known that both LDA and GGA xc potentials possess undesirable properties, of which their behavior in the outer region of the molecule is of crucial importance for response calculations. As the GGA and LDA xc potentials do not possess the correct Coulombic tail ($v_{xc} \rightarrow -1/r$), they systematically overestimate molecular polarizabilities. This overestimation increases if the outer region is more important for a particular system or for a particular effect. For this reason, the LDA works quite poorly for hyperpolarizabilities [32], higher multipole polarizabilities [29], high-lying excitation energies [38], and for small systems such as atoms. For large molecules, dipole polarizabilities, and low-lying excitation energies the LDA and GGA failure due to the incorrect asymptotics is less pronounced.

Substantial improvements can be obtained if the potentials are corrected in such a way that the proper asymptotic $-1/r$ behavior is restored. This can be done by using self-interaction correction (SIC) schemes, which have the disadvantage of making the potential orbital-dependent. A more popular choice has been the Van Leeuwen–Baerends model xc potential (LB94) [82], in which a simple local correction to the LDA potential is suggested. In spite of its simplicity, it corrects the LDA results in several important ways. An example of the influence of the correct asymptotics is given in Fig. 1, where the frequency-dependent quadrupole polarizability of Helium is plotted. Except for the benchmark ab initio curve, both the LDA/ALDA and LB94/ALDA results are shown. The LDA curve displays a clear overestimation of the static quadrupole polarizability, as well as a too steep frequency dependence, which is indicative of a too small value for the first relevant excitation energy. The LB94 curve shows important improvements in both the static value and in the frequency dependence.

These trends are by no means restricted to Helium. As demonstrated in Ref. [26], the LB94 potential removes the systematic LDA overestimation of molecular polarizabilities, as well as the LDA overestimation of the frequency dependence of these polarizabilities. In Ref. [29] it was shown that similar improvements are even more pronounced for the higher multipole polarizabilities and dispersion coefficients, which is

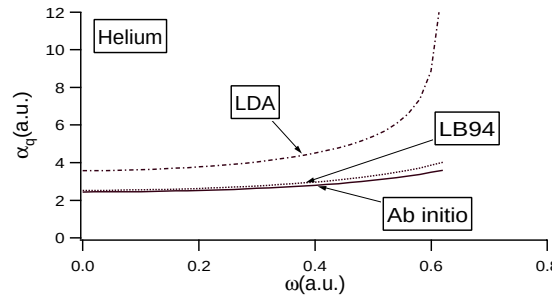

Fig. 1. The frequency-dependent quadrupole polarizability of He. Comparison of results with the LDA and LB94 potentials to benchmark ab initio results.

also the case for frequency-dependent hyperpolarizabilities [32]. Casida et al. [38] have recently shown that high-lying excitation energies are improved with respect to the LDA values if the LB94 potential is used. Similar improvements were obtained by Grabo et al. [83] with the KLI potential.

In a recent study [30] in which we used very accurate exchange correlation potentials, constructed from ab initio densities, it appeared that additional improvements for excitation energies and polarizabilities for atoms and small molecules can be expected from approximations to v_{xc} which are more accurate than the LB94 potential. In view of the relative simplicity of the LB94 potential, the construction of such an improved potential may be quite feasible. In fact, next to orbital-dependent functionals with correct asymptotics, such as the Krieger–Li–Iafrate (KLI) potential [84,85], new density functionals for accurate exchange-correlation potentials with correct asymptotics were recently proposed [86,87], and are awaiting to be tested in response calculations.

6.2. Excitation energies of small molecules

The first excitation energy calculations in TDDFT were performed by Petersilka and Gross [88,63,67,89] for atomic systems, and by Casida and Jamorski et al. [37,38] and Bauernschmitt and Ahlrichs [43–45] for molecules. As an example for the excitation energies of small molecules we give the results by Bauernschmitt and Ahlrichs for the lowest singlet and triplet excitation energies of the formaldehyde molecule in Table 1. Bauernschmitt and Ahlrichs [43] studied a set of several small molecules and concluded that the

Table 1
Excitation energies of CH_2O (in eV)

Transition		Excitation energy		
		LDA[a]	B3LYP [90,91][a]	Expt.
$^1B_1$	$\sigma \rightarrow \pi^*$	8.70	8.93	9.0
$^1A_1$	n$\rightarrow$ 3p	6.79	7.30	8.14
$^1B_2$	n$\rightarrow$ 3s	5.93	6.45	7.13
$^1A_2$	n$\rightarrow \pi^*$	3.64	3.88	4.1
$^3B_2$	n$\rightarrow$ 3s	5.86	6.32	7.09
$^3A_1$	$\pi \rightarrow \pi^*$	6.11	5.32	6.0
$^3A_2$	n$\rightarrow \pi^*$	3.02	3.14	3.5
Mean dev.		−0.70	−0.52	
Mean abs. dev.		0.74	0.52	

[a] Results taken from Ref. [43]. The CH_2O molecule has also been treated by Casida et al. [38].

B3LYP [90,91] functional gave the best performance of the methods studied (the LDA and Becke–Perdew potentials were slightly inferior, while the singles-CI and RPA results were clearly worse). The results in the table are typical in the sense that Bauernschmitt and Ahlrichs reported a systematic underestimation for the DFT excitation energies, with typical errors of 0.4 eV. Although these results provide clear improvements with respect to RPA or TDHF, it is still important to consider the origin of this underestimation, which incidentally corresponds to the overestimation in the polarizabilities. Bauernschmitt and Ahlrichs speculate that the adiabatic approximation may be largely responsible for this underestimation. This is contradicted however by the recent results of Casida et al. [38], which show that the use of the LB94 potential leads to much better values for high-lying excitation energies and to *overestimations* for low-lying molecular excitation energies. This shows at the same time that the LB94 potential needs to be improved upon and that the form of the xc potential, in particular its asymptotic behavior, is of considerable influence on the results for low-lying excitation energies as well.

In a more recent paper, Bauernschmitt et al. [44] have shown that excitation energies of large molecules can efficiently be obtained from a TDDFT approach. They provide timing results for calculations on molecules with up to about 80 atoms and 800 basis functions, which might be a good indication of what will be the magnitude of a standard calculation in the very near future, and is in agreement with our own experience for the C_{60} molecule [28] and polyene chains [33].

Very recently Bauernschmitt et al. [45] have applied TDDFT to the prediction of the electronic absorption of fullerenes. The excitation energy results are once more quite satisfactory, although again somewhat too low in comparison to experiment.

Apart from the TDDFT approach, excitation energies can also be calculated using ordinary ground-state DFT, through the so-called ΔSCF approach [3–6]. It is important to understand the characteristics of and differences between both types of calculation. For this reason, we have compared our own TDDFT calculations [80,92] for the prototype $Cr(CO)_6$ molecule to ΔSCF results which have appeared in the literature earlier. In Table 2, these DFT results are compared to experimental and ab initio complete active space second-order perturbation theory (CASPT2) results, which can be considered as the benchmark values in this case. All three theoretical approaches are in agreement about the assignment of the lowest excitation energies. They are of the charge transfer (CT) type, in disagreement with the longstanding accepted experimental assignment to the ligand field (LF) excitation [93], which therefore has to be reconsidered. In many cases, the ΔSCF and TDDFT results are (very) close to each other, but for some excitations there are remarkable differences of more than 1 eV, which cannot be attributed to basis set differences, as we have checked by performing TDDFT test calculations in identical basis and fit sets as were used in the ΔSCF calculations of Ref. [94] in which the ADF program was also used.

For example, the two CT excitations for which experimental numbers are available are predicted to be much lower by the TDDFT calculation than by the ΔSCF calculation. The TDDFT results are in much better agreement with the experimental and CASPT2 values than the ΔSCF values are.

We have found [80,92] that typically the ΔSCF and TDDFT results are close to each other in case the transition is dominated by one particular KS orbital replacement. In other words, if the eigenvector $\mathbf{F}_i$ in Eq. (24) belonging to the excitation energy has one dominant component, the ΔSCF and TDDFT approaches will yield very similar results. This is due to the fact that in the ΔSCF approach one can only con-

Table 2
Comparison of TDDFT and ΔSCF excitation energies of $Cr(CO)_6$ (in eV)

Symmetry	Transition[a]	Expt.[b]	ΔSCF[c]	TDDFT[d]	CASPT2[e]
Charge transfer excitations					
a^1T_{2u}	$2t_{2g} \rightarrow 9t_{1u}$		4.0	4.11	3.70–3.56
a^1E_u	$2t_{2g} \rightarrow 9t_{1u}$		4.0	4.08	3.41–3.59
a^1A_{2u}	$2t_{2g} \rightarrow 9t_{1u}$		4.2	4.56	3.58–3.58
b^1E_u	$2t_{2g} \rightarrow 2t_{2u}$		4.5	4.62	3.97–4.05
a^1A_{1u}	$2t_{2g} \rightarrow 2t_{2u}$		4.5	4.20	4.15–4.10
b^1T_{2u}	$2t_{2g} \rightarrow 2t_{2u}$		5.0	4.62	4.32–4.43
a^1T_{1u}	$2t_{2g} \rightarrow 9t_{1u}$	4.43	5.6	4.28	4.54–4.11
b^1T_{1u}	$2t_{2g} \rightarrow 2t_{2u}$	5.41	6.5	5.87	5.07–5.20
Ligand field excitations					
$^1T_{1g}$	$2t_{2g} \rightarrow 6e_g$		5.2	5.47	4.85
$^1T_{2g}$	$2t_{2g} \rightarrow 6e_g$		6.3	5.90	5.08

[a] For details about the orbital configuration, see Ref. [94].
[b] Experimental results from Ref. [102].
[c] Pollak et al. [94].
[d] Same basis sets were used as for ΔSCF calculations, BP potential [100,101] was used for ground-state calculation as in Ref. [94]. Results with larger basis sets or with the LDA potential differ by very small amounts [80].
[e] Complete active space second-order perturbation theory results with two different active spaces by Pierloot et al. [103].

sider a single orbital transition, and configuration interaction falls outside the scope of this approach, while it is included in a natural way in the TDDFT calculations. To give some numerical examples, we quote our results for the major components of the eigenvector for a few transitions. For the experimentally observed a^1T_{1u} and b^1T_{1u} transitions, the contribution of the major orbital transition is no larger than 64% and 58% respectively, if Casida's approximate assignment scheme is used [34]. In such cases, where there is considerable mixing between the orbital transitions, the ΔSCF results can deviate considerably. This observed trend needs to be investigated in more detail and should, at the moment, not be attributed more significance than a rule of thumb.

6.3. *Frequency-dependent hyperpolarizabilities*

TDDFT calculations may become particularly important for hyperpolarizabilities, as the frequency dependence is known to be large for this property. Atomic calculations for frequency-dependent hyperpolarizabilities were already performed a decade ago by Senatore and Subbaswamy [19,20]. More recently, analytic molecular calculations of static hyperpolarizabilities appeared [95,96]. Until now, only a single example [28] exists of a TDDFT calculation of a frequency-dependent hyperpolarizability of a molecular system, although a larger calibration study is in progress [32], as well as an application to the NLO response of polyene chains [33]. We have recently treated the C_{60} molecule in this approach [28], for which the first hyperpolarizability β is zero because of the high symmetry, making the second hyperpolarizability tensor γ the first nonvanishing nonlinear contribution.

The C_{60} molecule is an interesting case, because of its delocalized π-system, which led to speculations about its possibly huge hyperpolarizability, which would make it an interesting candidate for application in nonlinear optical devices. Our results [28], as well as various experimental and semiempirical results, have been gathered in Table 3 and Fig. 2. The disagreement between the experimental results is huge, and would be even larger if the older experimental results would have been included in the table. The semiempirical results seem to support the larger (and older) experimental values, although they are also very diverse. Both our LDA/ALDA and LB94/ALDA results give quite small values for the static hyperpolarizability tensor component γ_{zzzz} (which at zero frequency is equal to the average hyperpolarizability γ, because of the high symmetry of the molecule), which support the more recent experimental results by Geng and Wright [97], who could only estimate an upper limit for the hyperpolarizability. In addition, the frequency dependence we found was relatively small and could not explain the discrepancy with most experimental values. Very soon after the publication of our results, a static HF calculation on the hyperpolarizability appeared [98], which was in qualitative agreement with our results, thus providing strong support for both the DFT and HF calculations. Support has also come from new experimental results [99], giving low upper bounds for the hyperpolarizability of C_{60}.

Remaining differences between the experimental and theoretical values are in the neglect of solvent and vibrational effects in the theoretical description and form interesting subjects for future research.

Table 3
Experimental and theoretical results for γ of C_{60}

Method	ω(eV)	Property	γ (10^{-36} esu)
LB94[a]	0	static	5.50
LB94[a]	1.50	EOKE	6.69
LB94[a]	0.65	EFISH	6.04
LDA[a]	0	static	7.34
LDA[b]	0	static	7.0
INDO-TDHF[c]	0	static	4.95
INDO-TDHF[c]	0.905	EFISH	5.49
INDO/SDCI-SOS[d]	0.65	EFISH	690
CNDO/S[e]	0.94	THG	654.8
CNDO/SCI-SOS[f]	0	static	−458
Expt., in film[g]	0.68	THG	430
Expt., in toluene[h]	0.65	EFISH	750
Expt., in benzene[i]	1.17	DFWM	<60 $\times\gamma$(benzene)
Expt.[j]	various	Non-deg. FWM	<37

[a] Ref. [28].
[b] Quong and Pederson [104].
[c] Talapatra et al. [105].
[d] Li et al. [106].
[e] Hara et al. [107].
[f] Fanti et al. [108].
[g] Meth et al. [109].
[h] Wang and Cheng [110].
[i] Tang et al. [111], γ^{LDA}(benzene)$\approx 1.85\times10^{-36}$ esu [104].
[j] Geng and Wright [97], nondegenerate Four Wave Mixing experiment in 1,2-dichlorobenzene.

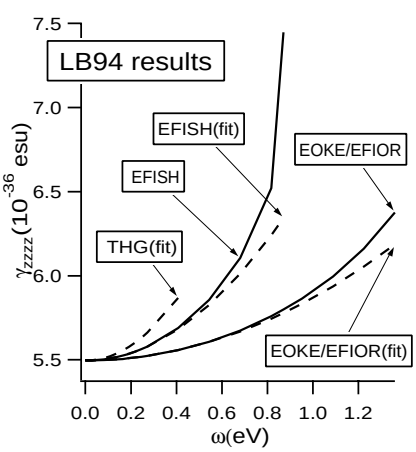

Fig. 2. LB94 results for γ of C_{60}.

6.4. Van der Waals dispersion coefficients

As mentioned before, the calculation of frequency-dependent multipole–multipole polarizabilities gives access to the Van der Waals dispersion coefficients which determine the long-range dispersion part of a potential energy surface of two interacting (distant) molecules. This is due to the fact that these dispersion coefficients can be calculated from an integral involving the polarizabilities at imaginary frequencies of the two monomers. If the distance R between the two subsystems becomes very large, the dominating term in the dispersion energy is of the form $-C_6/R^6$, where C_6 is the Van der Waals dispersion coefficient which can be calculated from the dipole–dipole polarizabilities of the monomers. At smaller distances, also the C_7 and C_8 coefficients become important, governing respectively the $-1/R^7$ and $-1/R^8$ behavior. For these coefficients, one needs, in addition to the dipole–dipole polarizabilities of the monomers, the dipole–quadrupole, and quadrupole–quadrupole polarizabilities. For the interaction between two centrosymmetric molecules, the C_7 coefficient vanishes because it depends on the vanishing dipole–quadrupole polarizability. In Table 4 we show results which we have obtained previously [29] for the C_8^0 coefficient, which governs the isotropic part of the $-1/R^8$ interaction between, in this case, a diatomic molecule and a rare gas atom. The basis sets which were used [29] were very large containing several diffuse functions, for which reason the results can be expected to be close to the basis set limit.

The LDA/ALDA and GGA/ALDA (using the Becke [100]–Perdew [101](BP) potential) results show the usual overestimations, which finally leads to average systematic errors of 20.5% and 13.2% with respect to the many-body perturbation theory (MBPT) values. The asymptotically correct LB94 potential largely corrects this, resulting in a much smaller error of 4.2%. The difference between the average and average absolute errors for the LB94 potential shows that for this potential the errors are not systematic.

For the relative anisotropy in the dispersion coefficients, satisfactory results were obtained with all three potentials mentioned above [29]. This implies that the difficult dispersion part of long-range potential energy surfaces can be constructed with useful accuracy from the described TDDFT approach.

Table 4
C_8^0 – Van der Waals coefficients for diatomic – rare gas interaction

Diatomic	Rare gas	LDA	BP	LB94	MBPT[a]	SoS[b]
H_2	He	77.31	67.13	59.74	53.60	55.38
H_2	Ne	167.6	153.5	133.7	128.4	
H_2	Ar	720.7	663.2	644.0	576.5	
H_2	Kr	1135	1051	989.5	953.6	
N_2	He	284.3	259.7	222.4	219.7	
N_2	Ne	599.1	574.2	481.4	498.7	
N_2	Ar	2334	2240	2068	1986	
N_2	Kr	3552	3429	3074	3145	
CO	He	334.0	304.9	257.9	262.7	
CO	Ne	693.6	664.2	548.9	588.9	
CO	Ar	2689	2576	2348	2355	
CO	Kr	4072	3923	3474	3726	
HCl	He	364.9	332.2	298.5	284.1	
HCl	Ne	764.5	730.6	639.8	643.7	
HCl	Ar	3048	2914	2815	2638	
HCl	Kr	4667	4487	4201	4219	
Cl_2	He	1026	946.1	849.4	810.3	
Cl_2	Ne	2086	2013	1758	1770	
Cl_2	Ar	7758	7479	7186	6764	
Cl_2	Kr	11539	11184	10439	10505	
Av. abs. error wrt MBPT		20.5%	13.2%	4.2%	–	
Av. error wrt MBPT		20.5%	13.2%	1.8%		

[a] Ref. [112] Many body perturbation theory, results were linearly interpolated.
[b] Ref. [113] Sum-over-states with explicitly electron-correlated wave functions (SoS).

7. Conclusions

After a brief summary of the key equations of time-dependent density functional response theory, we have described how the efficient solution of these response equations can take place. An efficient implementation rests on the iterative solution of the relevant equations for the polarizability and the excitation energies. The most time consuming part of such an iterative solution is formed by the repeated matrix–vector multiplications of the coupling matrix K with trial-vectors. Four important ingredients for the efficient evaluation of this matrix–vector multiplication have been discussed: the use of a density fit for the evaluation of the induced potential, the use of the molecular symmetry through the Wigner–Eckart theorem, the parallelization of the code, and the use of distance effects. With these techniques an efficient implementation of the time-dependent density functional response equations can be realized. Such an implementation allows for a first principles determination of excitation energies, frequency-dependent (hyper)polarizabilities, and related properties of large molecules. Work performed in other groups and by ourselves has shown that such calculations are usually of very satisfactory accuracy. A few calculations on polarizabilities, hyperpolarizabilities, excitation energies, and dispersion coefficients have been reviewed in order to give examples of what the theory can typically be used for, and what accuracy can be attained.

Acknowledgements

We would like to thank J.A. Groeneveld, F. Kootstra, and V.P. Osinga for the sizable contribution they have made to the implementation described in this work. SvG gratefully acknowledges financial support from the Netherlands organization for scientific research (NWO), through its foundations SON and NCF.

References

[1] P. Hohenberg, W. Kohn, Phys. Rev. 136 (1964) B864.
[2] W. Kohn, L.J. Sham, Phys. Rev. 140 (1965) A1133.
[3] T. Ziegler, A. Rauk, E.J. Baerends, Theoret. Chim. Acta 43 (1977) 261.
[4] U. von Barth, Phys. Rev. A 20 (1979) 1693.
[5] C. Daul, Int. J. Quantum Chem. 52 (1994) 867.
[6] R.M. Dickson, T. Ziegler, Int. J. Quantum Chem. 58 (1996) 681.
[7] T. Ando, Z. Phys. B 26 (1977) 263.
[8] A. Zangwill, P. Soven, Phys. Rev. A 21 (1980) 1561.
[9] A. Zangwill, P. Soven, Phys. Rev. Lett. 45 (1980) 204.
[10] A. Zangwill, P. Soven, Phys. Rev. B 24 (1981) 4121.
[11] A. Zangwill, J. Chem. Phys. 78 (1983) 5926.
[12] M.J. Stott, E. Zaremba, Phys. Rev. A 21 (1980) 12.
[13] S.K. Ghosh, B.M. Deb, Chem. Phys. 71 (1982) 295.
[14] S.K. Ghosh, B.M. Deb, Theoret. Chim. Acta 62 (1983) 209.
[15] Z.H. Levine, P. Soven, Phys. Rev. A 29 (1984) 625.
[16] G.D. Mahan, Phys. Rev. A 22 (1980) 1780.
[17] G.D. Mahan, J. Chem. Phys. 76 (1982) 493.
[18] K.R. Subbaswamy, G.D. Mahan, J. Chem. Phys. 84 (1986) 3317.
[19] G. Senatore, K.R. Subbaswamy, Phys. Rev. A 34 (1986) 3619.
[20] G. Senatore, K.R. Subbaswamy, Phys. Rev. A 35 (1987) 2440.
[21] G.D. Mahan, K.R. Subbaswamy, Local Density Theory of Polarizability (Plenum Press, New York, 1990).
[22] L.J. Bartolotti, J. Chem. Phys. 80 (1984) 5687.
[23] L.J. Bartolotti, L. Ortiz, Q. Xie, Int. J. Quantum Chem. 49 (1994) 449.
[24] E. Runge, E.K.U. Gross, Phys. Rev. Lett. 52 (1984) 997.
[25] S.J.A. van Gisbergen, J.G. Snijders, E.J. Baerends, J. Chem. Phys. 103 (1995) 9347.
[26] S.J.A. van Gisbergen, V.P. Osinga, O.V. Gritsenko, R. van Leeuwen, J.G. Snijders, E.J. Baerends, J. Chem. Phys. 105 (1996) 3142.
[27] S.J.A. van Gisbergen, J.G. Snijders, E.J. Baerends, Chem. Phys. Lett. 259 (1996) 599.
[28] S.J.A. van Gisbergen, J.G. Snijders, E.J. Baerends, Phys. Rev. Lett. 78 (1997) 3097.
[29] V.P. Osinga, S.J.A. van Gisbergen, J.G. Snijders, E.J. Baerends, J. Chem. Phys. 106 (1997) 5091.
[30] S.J.A. van Gisbergen, F. Kootstra, P.R.T. Schipper, O.V. Gritsenko, J.G. Snijders, E.J. Baerends, Phys. Rev. A 57 (1998) 2556.
[31] S.J.A. van Gisbergen, J.G. Snijders, E.J. Baerends, J. Chem. Phys. 109 (1998) 10644.
[32] S.J.A. van Gisbergen, J.G. Snijders, E.J. Baerends, J. Chem. Phys. 109 (1998) 10657.
[33] B. Champagne, E.A. Perpète, S.J.A. van Gisbergen, E.J. Baerends, J.G. Snijders, C. Soubra-Ghaoui, K. Robins, B. Kirtman, J. Chem. Phys. 109 (1998) 10489.
[34] M.E. Casida, in: Recent Advances in Density-Functional Methods, D.P. Chong, eds. (World Scientific, Singapore, 1995) p. 155.
[35] M.E. Casida, C. Jamorski, F. Bohr, J. Guan, D.R. Salahub, in: Theoretical and Computational Modeling of NLO and Electronic Materials, S.P. Karna, A.T. Yeates, eds. (ACS, Washington, DC, 1996) p. 145.
[36] M.E. Casida, in: Recent Developments and Applications of Modern Density Functional Theory, J.M. Seminario, ed. (Elsevier, Amsterdam, 1996).
[37] Ch. Jamorski, M.E. Casida, D.R. Salahub, J. Chem. Phys. 104 (1996) 5134.
[38] M.E. Casida, C. Jamorski, K.C. Casida, D.R. Salahub, J. Chem. Phys. 108 (1998) 4439.
[39] S.M. Colwell, N.C. Handy, A.M. Lee, Phys. Rev. A 53 (1996) 1316.
[40] A.G. Ioannou, S.M. Colwell, R.D. Amos, Chem. Phys. Lett. 278 (1997) 278.
[41] A.G. Ioannou, R.D. Amos, Chem. Phys. Lett. 279 (1997) 17.
[42] C. Van Caillie, R.D. Amos, Chem. Phys. Lett. 291 (1998) 71.
[43] R. Bauernschmitt, R. Ahlrichs, Chem. Phys. Lett. 256 (1996) 454.
[44] R. Bauernschmitt, M. Häser, O. Treutler, R. Ahlrichs, Chem. Phys. Lett. 264 (1997) 573.
[45] R. Bauernschmitt, R. Ahlrichs, F.H. Hennrich, M.K. Kappes, J. Am. Chem. Soc. 120 (1998) 5052.
[46] RESPONSE, extension of the ADF program for linear and nonlinear response calculations, by S.J.A. van Gisbergen, J.G. Snijders, E.J. Baerends, with contributions by J.A. Groeneveld, F. Kootstra, V.P. Osinga.
[47] E.J. Baerends, D.E. Ellis, P. Ros, Chem. Phys. 2 (1973) 41.
[48] G. te Velde, E.J. Baerends, J. Comput. Phys. 99 (1992) 84.
[49] C. Fonseca Guerra, O. Visser, J.G. Snijders, G. te Velde, E.J. Baerends, in: Methods and Techniques in Computational Chemistry, E. Clementi, G. Corongiu, eds. (STEF, Cagliari, Italy, 1995) p. 305.
[50] H. Hellmann, Einführung in die Quantenchemie (Franz Deutiche, Leipzig, 1937).
[51] R.P. Feynman, Phys. Rev. 56 (1939) 340.
[52] A. Willetts, J.E. Rice, D.M. Burland, D.P. Shelton, J. Chem. Phys. 97 (1992) 7590.
[53] P. Craig, T. Thirunamachandran, Molecular Quantum Electrodynamics (Academic Press, New York, 1984).
[54] P. Pulay, Chem. Phys. Lett. 73 (1980) 393.
[55] P. Pulay, J. Comput. Chem. 3 (1982) 556.
[56] C-A. Ullrich, Time-dependent density-functional approach to atoms in strong laser pulses, Ph.D. thesis, Universität Würzburg (1995).
[57] C.A. Ullrich, U.J. Gossmann, E.K.U. Gross, Phys. Rev. Lett. 74 (1995) 872.
[58] E.K.U. Gross, J.F. Dobson, M. Petersilka, in: Density Functional Theory, Springer Series Topics in Current Chemistry, R.F. Nalewajski, ed. (Springer, Heidelberg, 1996).
[59] Xiao-Min Tong, Shih-I Chu, Phys. Rev. A 57 (1998) 452.
[60] E.K.U. Gross, W. Kohn, Adv. Quantum Chem. 21 (1990) 255.

[61] E.K.U. Gross, C.A. Ullrich, U.J. Gossmann, Density Functional Theory of Time-Dependent Systems, NATO ASI Ser. B, Vol. 337 (Plenum Press, New York, 1995) p. 149.
[62] J.G. Snijders, internal report, Vrije Universiteit, Amsterdam.
[63] M. Petersilka, U.J. Gossmann, E.K.U. Gross, Phys. Rev. Lett. 76 (1996) 1212.
[64] R. McWeeny, Methods of Molecular Quantum Mechanics (Academic Press, New York, 1990).
[65] P. Jørgensen, J. Simons, Second Quantization-Based Methods in Quantum Chemistry (Academic Press, New York, 1981).
[66] S.P. Karna, M. Dupuis, J. Comput. Chem. 12 (1991) 487.
[67] M. Petersilka, E.K.U. Gross, Int. J. Quantum Chem. Symp. 30 (1996) 181.
[68] K.L. Liu, S.H. Vosko, Can. J. Phys. 67 (1989) 1015.
[69] K.L. Liu, Can. J. Phys. 69 (1991) 573.
[70] J. Olsen, H.J.Aa. Jensen, P. Jørgensen, J. Comput. Phys. 74 (1988) 265.
[71] E.R. Davidson, J. Comput. Phys. 17 (1975) 87.
[72] B. Liu, Proc. Numerical Algorithms in Chemistry: Algebraic Methods, Workshop of the National Resource for Computation in Chemistry, Berkeley (1978) p. 49.
[73] E.R. Davidson, Comput. Phys. 7 (1993).
[74] A. Stathopoulos, C.F. Fischer, Comput. Phys. Commun. 79 (1994) 268.
[75] A. Savin, C.J. Umrigar, X. Gonze, Chem. Phys. Lett. 288 (1998) 391.
[76] C. Fonseca Guerra, J.G. Snijders, G. te Velde, E.J. Baerends, Theor. Chem. Acc. 99 (1998) 391.
[77] P.M. Boerrigter, G. te Velde, E.J. Baerends, Int. J. Quantum Chem. 33 (1988) 87.
[78] G. te Velde. Ph.D. thesis, Vrije Universiteit, Amsterdam, The Netherlands (1990).
[79] J.F. Cornwelll, Group Theory in Physics (Academic Press, New York, 1984).
[80] J.A. Groeneveld, internal report, Vrije Universiteit, Amsterdam (1998).
[81] V. Sunderam, Concurrency: Practice Experience 2(4) (1990).
[82] R. van Leeuwen, E.J. Baerends, Phys. Rev. A 49 (1994) 2421.
[83] T. Grabo. Orbital dependent functionals in density functional theory, Ph.D. thesis, University of Würzburg (1997).
[84] J.B. Krieger, Y. Li, G.J. Iafrate, Phys. Rev. A 46 (1992) 5453.
[85] Y. Li, J.B. Krieger, G.J. Iafrate, Phys. Rev. A 47 (1993) 165.
[86] D.J. Tozer, N.C. Handy, J. Chem. Phys. 108 (1998) 2545.
[87] M. Filatov, W. Thiel, Phys. Rev. A 57 (1998) 189.
[88] M. Petersilka, Diplomarbeit, Universität Würzburg (1993).
[89] M. Petersilka, U.J. Gossmann, E.K.U. Gross, in: Electronic Density Functional Theory: Recent Progress and New Directions, J.F. Dobson, G. Vignale, M.P. Das, eds. (Plenum Press, New York, 1998) pp. 177–197.
[90] A.D. Becke, J. Chem. Phys. 98 (1988) 5648.
[91] C. Lee, W. Yang, R.G. Parr, Phys. Rev. B 37 (1988) 785.
[92] A. Rosa, E.J. Baerends, S.J.A. van Gisbergen, E. van Lenthe, J.A. Groeneveld, J.G. Snijders, submitted.
[93] N.A. Beach, H.B. Gray, J. Am. Chem. Soc. 90 (1968) 5731.
[94] C. Pollak, A. Rosa, E.J. Baerends, J. Am. Chem. Soc. 119 (1997) 7324.
[95] S.M. Colwell, C.W. Murray, N.C. Handy, R.D. Amos, Chem. Phys. Lett. 210 (1993) 261.
[96] A.M. Lee, S.M. Colwell, J. Chem. Phys. 101 (1994) 9704.
[97] L. Geng, J.C. Wright, Chem. Phys. Lett. 249 (1996) 105.
[98] P. Norman, Y. Luo, D. Jonsson, H. Ågren, J. Chem. Phys. 106 (1997) 8788.
[99] Jianliang Li, Shufeng Wang, Hong Yang, Qihuang Gong, Xin An, Huiying Chen, Di Qiang, Chem. Phys. Lett. 288 (1998) 175.
[100] A.D. Becke, Phys. Rev. A 38 (1988) 3098.
[101] J.P. Perdew, Phys. Rev. B 33 (1986) 8822.
[102] H.B. Gray, N.A. Beach, J. Am. Chem. Soc. 85 (1963) 2922.
[103] K. Pierloot, E. Tsokos, L.G. Vanquickenborne, J. Phys. Chem. 100 (1996) 16545.
[104] A.A. Quong, M.R. Pederson, Phys. Rev. B 46 (1992) 12906.
[105] G.B. Talapatra, N. Manickam, M. Samoc, M.E. Orczyk, S.P. Karna, P.N. Prasad, J. Phys. Chem. 96 (1992) 5206.
[106] J. Li, J. Feng, C. Sun, Chem. Phys. Lett. 203 (1993) 560.
[107] T. Hara, Y. Nomura, S. Narita, T. Shibuya, Chem. Phys. Lett. 240 (1995) 610.
[108] M. Fanti, G. Orlandi, F. Zerbetto, J. Am. Chem. Soc. 117 (1995) 6101.
[109] J.S. Meth, H. Vanherzeele, Y. Wang, Chem. Phys. Lett. 197 (1992) 26.
[110] Y. Wang, L-.T. Cheng, J. Phys. Chem. 96 (1992) 1530.
[111] N. Tang, J.P. Partanen, R.W. Hellwarth, R.J. Knize, Phys. Rev. B 48 (1993) 8404.
[112] H. Hettema, P.E.S. Wormer, A.J. Thakkar, Mol. Phys. 80 (1993) 533.
[113] D.M. Bishop, J. Pipin, Int. J. Quantum Chem. 45 (1993) 349.